Hierarchical construction of self-assembled low-dimensional molecular architectures observed by using scanning tunneling microscopy

Yanlian Yang and Chen Wang*

Received 9th January 2009
First published as an Advance Article on the web 26th June 2009
DOI: 10.1039/b807500j

This *tutorial review* is intended to reflect the progress in constructing functional low-dimensional molecular nanostructures on surfaces through hierarchical self-assembly processes. Hierarchical assembly can be characterized as a multilevel process, and represented by categories depending on symmetry characteristics and the nature of intermolecular interactions. Various approaches have been explored in order to gain knowledge on tailoring hierarchical assembly characteristics, driving mechanisms and designing principles. The advances in hierarchical assembly structures could benefit the efforts towards constructing well-defined molecular architectures, which are important to the development of novel material properties and molecular devices.

1. Introduction

Hierarchical molecular assembly has drawn increasing interest in recent years because of the possibility of fabricating highly ordered functional superstructures from elemental building units. The multilevel assembling process is initiated by the assembly of elemental building units into clusters *via* non-covalent interactions. Subsequently, these molecular clusters become the building blocks to form more complicated assembling structures.

Hierarchical assembly exists abundantly in biological systems as well as in synthetic molecules or nanomaterials that could facilitate the formation of well-defined functional aggregates without synthesizing the whole structure bond-by-bond. Two-dimensional (2D) and three-dimensional (3D) hierarchical assemblies have been demonstrated for constructing functional materials, devices or systems, ranging from the assembly of DNA,[1] peptides,[2] π-conjugated molecules[3,4] and related block copolymers,[5] to name a few. As one of the promising aspects of nanoscience and nanotechnology, hierarchical assembly has been extensively pursued in recent years, not only in 3D materials and structures, but also in the construction of 2D surface molecular nanostructures. Molecular scale structural information obtained by techniques such as scanning tunneling microscopy (STM) is considered key to understanding the mechanisms governing the assembly processes. A rich variety of ordered 2D molecular assemblies have been observed with the aid of STM and many other surface characterization techniques. The unique capability of STM working in various environments has enabled systematic investigations of the molecule–molecule and molecule–substrate interactions. Ultra-high vacuum (UHV) conditions can provide well-defined environments for studying the evidence of such interactions.

National Center for Nanoscience and Technology, Beijing, 100190, China. E-mail: wangch@nanoctr.cn

Yanlian Yang

Y. L. Yang received BS and MS degrees in Chemistry from Shandong University in 1996 and 1999, respectively. In 2002, she obtained a PhD degree in physical chemistry from Peking University, and was then a postdoctoral researcher in Peking University from 2002 to 2004. She was a visiting scholar at the Center for Biomedical Engineering, Massachusetts Institute of Technology from 2007 to 2008. She currently is an associate professor in the National Center for Nanoscience and Technology of China. Her research interests include molecular and nanomaterial self-assembly, and the physical and chemical properties of single molecules.

Chen Wang

C. Wang received a BS degree from the University of Science and Technology of China in 1986. After this, he obtained his PhD from the University of Virginia in 1992 and he joined Arizona State University as a postdoctoral associate. In 1994, he became a professor of Central China Normal University. He was a faculty of the Institute of Chemistry, CAS from 1995 to 2004, and is currently a professor and director of National Center for Nanoscience and Technology of China. He has engaged in studies of scanning tunneling microscopy/spectroscopy and its applications, including molecular self-assembly, and the physical and chemical properties of single molecules, etc.

Complementary studies at solution–solid interfaces provide additional insights into possible solvent effects and adsorption–desorption dynamic processes in the assembly characteristics of molecular architectures. Several reviews have discussed molecular designs and assembly mechanisms, as well as associated solvent or thermal effects on molecular assemblies for a variety of alkyl derivatives, macrocyclic molecules, hydrogen-bonded supramolecular networks, metal–organic coordination connected nanoporous networks and host–guest architectures.[6–9]

Hierarchical molecular assembly on surfaces shows a promising potential for the rational design of supramolecular structures with high complexity and reversibility. It is still challenging to fully understand the principles governing the transition from elemental building units to higher level assemblies and even macroscopic systems. The mechanism governing the hierarchical structure formation on surfaces should include the interplay of non-covalent molecule–molecule and molecule–substrate interactions, and also the interplay of interactions with different strengths.

We will review in this work a series of molecular nanostructures starting from elemental units to hierarchical molecular structures, in which the molecular species could be studied at the level of single molecules and single clusters. The evolution of hierarchical molecular architectures is associated with the co-existence of multiple interactions at different levels.[10] The reported elemental building units include a variety of species, such as aromatic molecules connected by hydrogen bonds or metal–organic coordination interactions, *etc*. It should be noted that the interaction strength between basic units at the starting level is usually stronger than that between the building blocks at higher levels.

The assembly characteristics of the hierarchical assemblies with similar structural symmetries at different levels are reviewed at first, followed by the hierarchical molecular structures with dissimilar structural symmetries at different levels. The environmental effects on the hierarchical assemblies are also discussed including substrate, solvent and thermal effects, *etc*. We will discuss the assembly characteristics in light of decreasing interaction strength with hierarchy levels throughout the review.

2. Hierarchical assembly with similar symmetries

The hierarchical assembly of molecules reflects intrinsic characteristics (functional groups, molecular symmetry, dipole moment, *etc*.) encoded in the individual elemental building units.[11] Hierarchical assembly with similar structural symmetries for molecular clusters and higher level assemblies could be ascribed to symmetrically distributed interactions, and the interaction strength is decreasing with the increase of the hierarchical levels. In case of an elemental molecular building unit, schematically represented by a triangular structure as illustrated in Scheme 1a, the dominant interactions between the apexes of four molecules result in square-shaped clusters or secondary building blocks. Subsequent assembling of the square-shaped clusters into square-shaped arrays is dominated by the weak interactions between the sides or the corner points of the square-shaped building blocks. Assemblies with similar

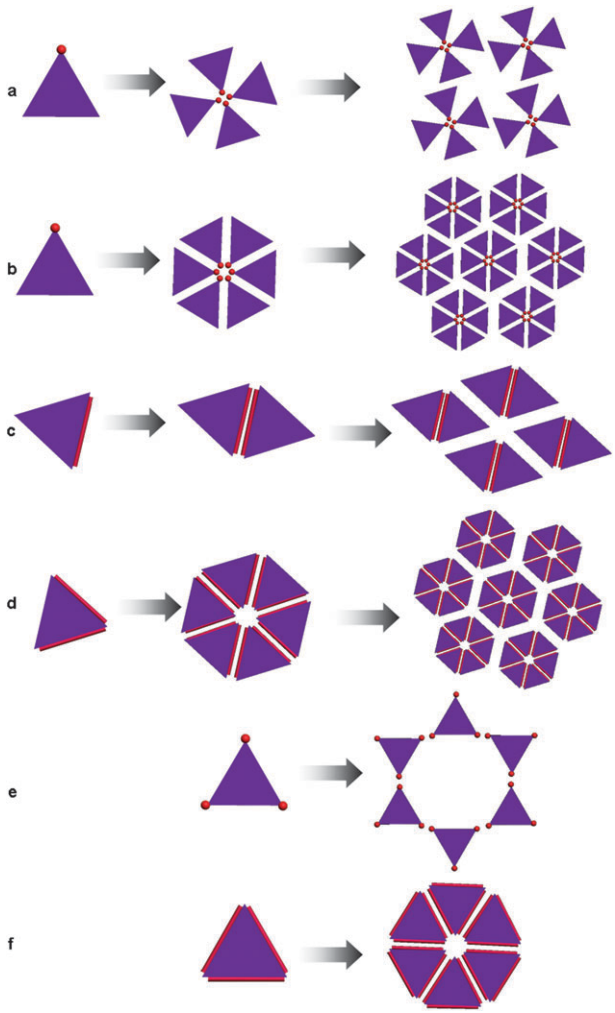

Scheme 1 Schematic illustrations of hierarchical assemblies with similar symmetries at different levels. The elemental molecular building unit is schematically represented by a triangular structure and the dominant interaction sites are schematically presented by red spheres for interactions at corner points, and red rods for interactions at sides. (a) The dominant interactions between the apexes of four triangles result in square-shaped clusters or secondary building blocks, and then subsequent assembling into square-shaped arrays dominated by weak interactions between the sides of the square-shaped building blocks. (b) and (d) Hexagonal hierarchical assemblies with the dominant interactions between one point (b) or two sides (d), respectively. (c) Rhombic hierarchical assemblies with dominant interactions between sides. (e) Hexagonal hierarchical arrangement with a cavity inside of the network assembled from triangular building blocks with relatively strong interaction sites located on three corner points. (f) Hexagonal hierarchical arrangement from close-packing of triangular building blocks with relatively strong interactions between all three sides. It should be noted that for both of the two cases illustrated in (e) and (f), the triangular structures are clusters assembled from elemental building units.

symmetry at different levels are illustrated in Schemes 1a–f. Hexagonal hierarchical assemblies could be associated with dominant interactions between corner points (Scheme 1b) or two sides (Scheme 1d) of the triangular structure. Rhombic hierarchical assemblies could be associated with dominant interactions between sides of the triangular structure

(Scheme 1c). The hexagonal hierarchical arrangement, with a cavity inside of the network, is shown in Scheme 1e, with relatively strong interaction sites located on three corner points of the triangular building blocks. Another type of hierarchical assembly could be evolved from the close-packing of triangular building blocks into a hexagonal arrangement due to relatively strong interactions between all three sides of the triangular structure (Scheme 1f). It should be noted that for both of the two cases illustrated in Schemes 1e and f, the triangular structures are clusters assembled from elemental building units. The similarity in structural symmetry at different levels illustrates the hierarchical process for assembling molecular clusters, which will be discussed in this section. The discussion here will also reflect the difference in the interaction strength at different hierarchical levels.

2.1 Hierarchical assembly with van der Waals interactions at the first level

Van der Waals interactions are a kind of non-covalent weak interactions without specificity or directionality, but it is crucial for molecular assemblies on surfaces, especially for molecules with alkyl substituents. Other non-directional interactions such as steric interactions, electrostatic interactions, dipole–dipole interactions, *etc.*, also play important roles in hierarchical assemblies on surface. The incorporation of these non-directional interactions will render the assembly characteristics appreciably more complex. Here we take van der Waals interactions as an example for illustration of the hierarchical assembly based on non-directional interactions.

Van der Waals interactions at both levels with the decreasing interaction strength could be applied for the hierarchical assemblies. A series of molecules were designed based on a 2,4,6-tristyrylpyridine core for the formation of strong surface-assisted intermolecular "clips" by interdigitation of *n*-alkanes on a highly oriented pyralytic graphite (HOPG) surface.[12] As anticipated, mono-functionalized molecules (mono-clips) form supramolecular dimers through the close-packing of alkyl chains at one side of the triangular molecules. At the second level, the parallelogram formed by the dimer of the mono-clip was assembled through van der Waals interactions between the non-functionalized styryl groups. The parallelogram-shaped packing of the parallelogram dimers follows the hierarchical assembly model shown in Scheme 1c.

2.2 Hierarchical assembly with hydrogen bond interactions at the first level

It is well known that hydrogen bonding is one of the key driving interactions for self-assembled molecular structures, especially for biomolecules and biomimetic systems. Various self-assembled patterns can be achieved through different types of hydrogen bonds, or hydrogen bonds together with van der Waals interactions. In this section, hierarchical assembly with hydrogen bonds as the dominant interaction are discussed, associated with hydrogen bonds or van der Waals interactions at the second level.

Hierarchical assembly with hydrogen bonds and van der Waals interactions. A variety of studies have been reported on controlled assembly behavior with the aid of directional interactions of hydrogen bonds. Dendrimers, having cores with a few functional groups to which a number of dendrons (dendritic wedges) are attached, are a widely studied class of compounds. The shape and size of a dendrimer governed by the architecture of the dendrons, core functionalities and the generation numbers are determining factors for the shapes and symmetries of the hierarchical assemblies. Several hierarchical assemblies of low generation dendrimers have been observed, predominantly with hydrogen bonds at the first level and van der Waals interactions at the higher level.[13–15] The self-assembled structures of monodendron **1** with a carboxylic acid group at the focal point display rhombic symmetry at both levels (Fig. 1a and e),[13] similar to Scheme 1a. Similarly to monodendron **1**, rhombic hierarchical features at both levels were also observed at the liquid–solid interface for monodendron **2** possessing 2nd generation structure (Fig. 1b and f).[14] Furthermore, it is interesting to note that in hydrophobic solvating solvents, such as aliphatic and aromatic hydrocarbons, solvent molecules could coadsorb in the 2D molecular network.[14] For monodendron **3** with a carboxylic acid group at the focal point,[15] similar to Scheme 1b, hydrogen bonds between the O–H and C=O groups of neighboring molecules lead to the hexagonal disk-like structures. The higher level assembly is dominated by close-packing of hexagonal disk-like structures *via* van der Waals interactions (Fig. 1c and g). Whereas for monodendron **4**, with an ester group at the focal point (Fig. 1d and h),[15] the dipole–dipole interactions between ester groups are very weak, and the steric hindrance between methyl groups at the focal points is large. These two factors, together with the maximization of the contacts between aromatic groups, lead to the ordered assembly structure similar to Scheme 1c. These examples indicate that hydrogen bonds at the focal points are the driving forces for the formation of tetramers or hexamers at the first level, with distinctive structural symmetries. The 2D assembly of the building blocks at higher levels approximately replicates the structural symmetry of the molecular arrangements in the building blocks.

From the above investigations on a series of monodendron molecules with –COOH groups at the focal points, one could propose that the clustering of the molecules at the first level is steered by hydrogen bond formation between the –COOH groups. The peripheral shapes of the hydrogen-bonded monodendron clusters are dependent on the distribution of van der Waals interactions associated with alkyl substitutions. For monodendrons **1** and **2**, the crystallization of the alkyl chains leads to the square- or rhombic-shaped building blocks, while a similar distribution of van der Waals interactions at all of the three triangular sides for monodendron **3** gives rise to the hexagonal networks consisting of close-packed triangles.

Hydrogen bond interactions at both levels with decreasing strength. Aromatic molecules with specific symmetry and functionality have been widely pursued as the starting structures in hierarchical assembly processes. The hydrogen bond is a vital interaction in hierarchical assemblies for its specificity and directionality. The elemental building unit of oligopyridine, 2-phenyl-4,6-bis(6-(pyridine-3-yl)-4-(pyridine-3-yl)-pyridine-2-yl) pyrimidine (3,3′-BTP) forms a polymorphic supramolecular hydrogen-bonded network on a graphite

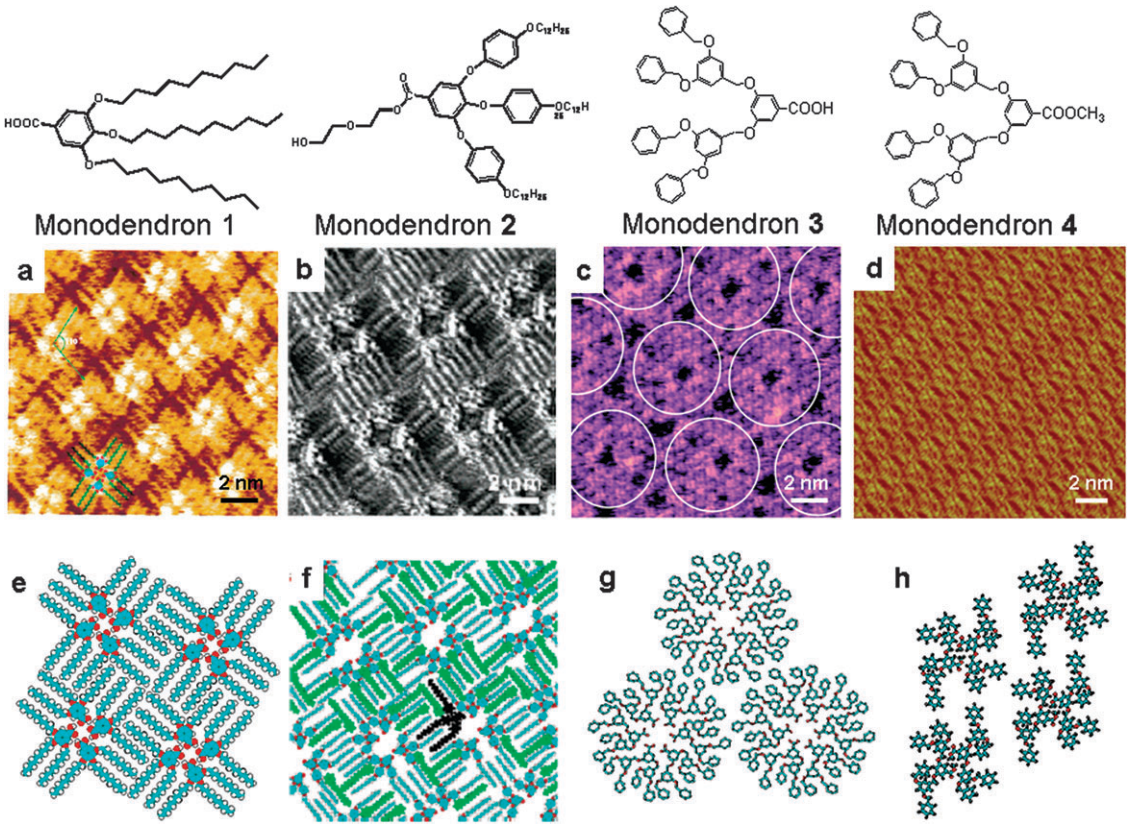

Fig. 1 (a–d) STM images of hierarchical assemblies of a series of monodendrons, **1**, **2**, **3** and **4**, respectively. The molecular structures of the monodendrons are presented correspondingly. Monodendrons **1**, **3** and **4** are physisorbed on a graphite surface under ambient conditions, and monodendron **2** is physisorbed at the 1-phenyltetradecane–graphite interface. (e–h) Tentative molecular models for corresponding hierarchical assembly of monodendrons **1**, **2**, **3** and **4**, respectively. The molecular structure of monodendron **2** is highlighted in the molecular model in (f) for guidance of the eyes. (a and e, reproduced with permission from ref. 13, copyright 2002 American Chemical Society; b and f, reproduced with permission from ref. 14, copyright 2006 American Chemical Society; c, d, g and h, reproduced with permission from ref. 15, copyright 2002 Wiley-VCH Verlag GmbH & Co. KGaA).

surface.[16] Deposited from a diluted solution (3×10^{-5} mol L^{-1}), the 3,3′-BTP molecules self-assemble into an ordered 2D porous nanostructure, with an inner pore size of 1.4 nm denoted as a gearwheel structure. At the first level, the building blocks are self-assembled from six 3,3′-BTP molecules into hexagonal porous clusters stabilized through N···H–C hydrogen bonds between terminal pyridyls at both sides (Fig. 2a). This assembly feature is similar to the mechanism proposed in Scheme 1d, in which two sides of the triangles are connected by hydrogen bonds into hexagonal building blocks. At the higher level, the replication of the symmetry of the building blocks leads to hexagonal networks through N···H–C hydrogen bonds with lower densities, together with the van der Waals interactions between benzene groups. This hierarchical network was shown to be capable of immobilizing guest molecules, such as copper phthalocyanine (CuPc), or 3,3′-BTP molecules.

Another example is the hierarchical assembly of guanine molecules on an Au(111) surface under UHV conditions.[17] The guanine (G) molecules appear as triangles in the STM image, and the first level arrangement of the triangle through two C═O···H–N and two N–H···N hydrogen bonds leads to the G-quartet structure with chirality. The G-quartet Hoogsteen-bonded structures, well-known in G-quadruplex in solutions, are assembled at a higher level, with a similar symmetry of quasi-square characteristics (Fig. 2b). This assembling scenario can be considered as similar to the one shown in Scheme 1a, while the building blocks are rotated with an angle of nearly 45°.

A heterogeneous network structure can be achieved by co-deposition of melamine (M) molecules with cyanuric acid (CA) molecules on an Au(111) surface.[18] Simultaneous deposition of CA and M leads to CA_1M_1 assembly, in which a heterodimer is formed through one N–H···N and two N–H···O hydrogen bonds. Furthermore, if CA is deposited after M, CA_1M_3 networks will be obtained. In this CA_1M_3 network, the building blocks with triangular shapes contain binary species connected by three hydrogen bonds between CA and M molecules. At the second level of assembly, the triangular building blocks are assembled into hexagonal hydrogen-bonded networks by two N–H···N hydrogen bonds between outer melamine molecules. The hydrogen bond density decreasing with assembly levels gives rise to the hierarchical assembly from the complementary hydrogen-bonded motifs. The second level assembly follows the characteristics shown in Scheme 1f, which is associated with nearly identical interaction strength at three sides of the triangular structure.

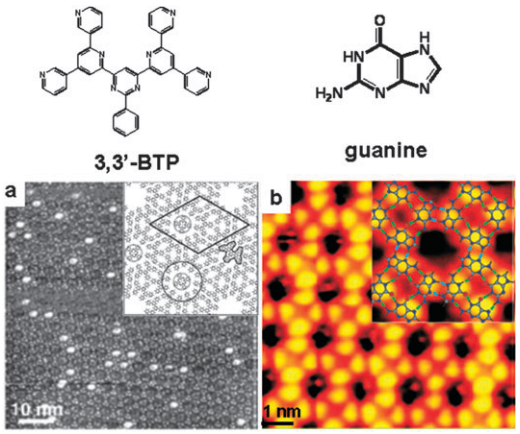

Fig. 2 Hierarchical assemblies with hydrogen bonds at both levels. (a) High-resolution STM image of the host–guest network recorded after addition of copper phthalocyanine to the 3,3′-BTP (molecular structure is presented above the STM image) network. The inset of (a) is the molecular structure of the host–guest network and the rhombic unit cell. A single gearwheel is highlighted with a black circle. A 3,3′-BTP molecule incorporated as guest is outlined in black. Copper phthalocyanine in its three energetically equivalent adsorption configurations is highlighted by dashed circles. (Reproduced with permission from ref. 16. Copyright 2008 Wiley-VCH Verlag GmbH & Co. KGaA.) (b) STM image showing that the guanine (molecular structure is presented above the STM image) network has an almost square geometry. The inset of (b) is the comparison of an STM image of G-quartet unit cells with the relaxed structure obtained by DFT calculations. The intraquartet hydrogen bonds are shown in green; interquartet hydrogen bonds, in blue. (Reproduced with permission from ref. 17. Copyright 2005 Wiley-VCH Verlag GmbH & Co. KGaA).

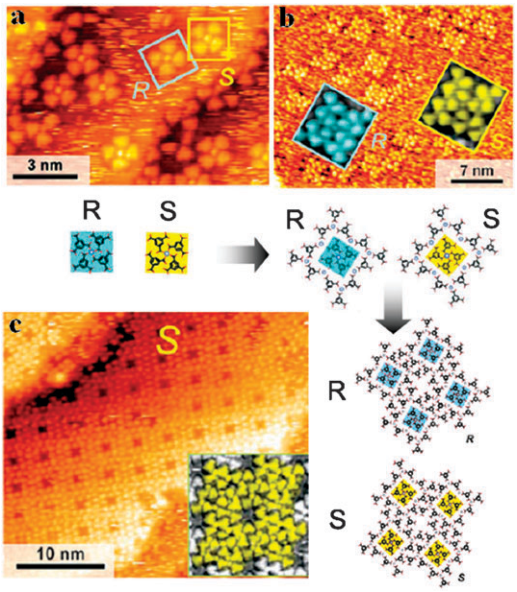

Fig. 3 (a–c) Sequential assembly of square-shaped Fe–TMA nanogrids on Cu(100), from (a) the mononuclear Fe–TMA_4 clusters, which are nuclei for the assembly of Fe–TMA nanogrids, (b) square-shaped polynuclear nanogrids, which are building blocks for the (c) porous nanogrid array structures. The insets in (b) and (c) highlight details of the molecular arrangement. The models illustrate the two mirror-symmetric representations labeled *R* and *S*, respectively, which exist at all levels. (Reproduced with permission from ref. 20. Copyright 2003 American Chemical Society, and permission from Annual Reviews. Molecular Architectonic on Metal Surfaces, J. V. Barth, *Annu. Rev. Phys. Chem.*, 2007, **58**, 375–407, Copyright 2007 Annual Reviews).

2.3 Hierarchical assembly with metal-coordination interaction at the first level

The high directionality and strength of metal–organic coordination interactions facilitate the rational design of low dimensional molecular assemblies, especially multilevel hierarchical structures for more complicated heterogeneous molecular architectures with functionality. Much effort has been given to the identification and control of hierarchical organization of metal–organic coordination networks on metal surfaces. Based on the chiral square-shaped complexes of 1,2,4-benzenetricarboxylic acid (tmla) and iron, large homochiral metal–organic arrays were demonstrated with a distinctive multilevel process.[19] The interactions at the higher hierarchical level are ascribed to coupling of the anionic carboxylate groups at the exterior of the cloverleafs to the aromatic rings of adjacent $Fe(tmla)_4$, through hydrogen bonds or weak electrostatic forces, which are lower in strength than metal–organic coordination at the first level. Such a hierarchical assembly feature is similar to the one shown in Scheme 1a, in which the determining interactions at both levels are located at the corner points. The chiroselective interaction also plays an important role in the formation of the superstructure. The symmetry breaking because of the folding of the individual complex results in the initial chirality signature of a domain and subsequent chirality proliferation for homochiral array formations.

Nanoporous 2D supramolecular structures formed by the hierarchical assembly of organic molecules up to three levels are demonstrated for 1,3,5-benzenetricarboxylic acid (trimesic acid, TMA) molecules and Fe atoms.[20] Rational design of the hierarchical assembly at different levels can be achieved by tuning the molecular stoichiometry and annealing temperature of the substrate. From the elemental components, the mononuclear chiral complexes are formed through metal–organic coordination interactions at the first level (Fig. 3a), which are the building blocks for the polynuclear metal–organic nanogrids connected by further coordination interactions (Fig. 3b). At the second level of the assembly, the coordination number of Fe is reduced from 4 to 3, which means that the overall interaction strength is also reduced accordingly. The nanogrids are eventually connected by hydrogen bonds at the third hierarchical level, leading to 2D networks (Fig. 3c). This demonstration in obtaining structures with increasing complexity could give rise to promising venues for studying 2D homogeneous and heterogeneous catalysis.[21]

The hierarchical assembly of a honeycomb-structured network of bis(terpyridine)-functionalized perylene tetracarboxylic bisimide[22] can be constructed with the trimeric macrocycle connected with Zn^{2+}-bis(terpyridine) coordination. The hexagonal arrangement at the second level of hierarchy is associated with the interaction of the aliphatic side chains of the adjacent macrocycles. This assembly feature can be illustrated by strong interactions located at the three corner points of the triangle apexes leading to hexagonal arrangement with cavities inside of the network (Scheme 1e). This hierarchical organization of the macrocycles showed

structural organization reminiscent of cyclic dye arrays in the purple bacterial photosynthetic membrane.[22]

2.4 Template-assisted hierarchical assembly

The 2D assembly process of multi-component molecular systems has attracted much attention because of the rich variety for designing molecular structures. A molecular template formed at the first level could incorporate guest molecules with high structural specificity. This kind of host–guest assembly may also be considered as a secondary level of hierarchical assembly. The construction of various host–guest molecular architectures could enable possible property tailoring by exchanging candidate guest species in the guest–host complexes. This latter topic is beyond the scope of this review but can be found in a number of other reviews.[6,7,23]

Replicate template with rigid structures. Many of the reported networks stabilized by hydrogen bonds or van der Waals interactions consist of large cavities, providing a rich ground for the exploration of composite molecular architectures. The highly ordered and porous 2D hydrogen-bonded hexagonal networks have been reported by adsorption of molecules with aromatic moieties, such as TMA adsorbed on a Cu(100)[24] or graphite surface.[25] Site-specific interaction of guest molecular species with the host assembly could lead to replication of the structural characteristics of the host. As an example, large areas of a hydrogen-bonded molecular network formed by perylenetetracarboxylic-diimide (PTCDI) and melamine were obtained on an Ag/Si(111)-$\sqrt{3} \times \sqrt{3}$ R30° surface under UHV conditions.[26] Such a supramolecular network adopts a hexagonal pattern with a lattice constant of 34.6 Å. The C_{60} molecules can adsorb directly on top of PTCDI and melamine molecules, leading to a replicated lattice structure. In addition, up to seven C_{60} molecules could be included in the cavities of the binary supramolecular networks.

Template replication can also be achieved by charge-transfer interactions between the host lattice and guest molecules.[27,28] The epitaxial growth of 3D C_{60} architectures was demonstrated with highly ordered monolayers of macrocyclic oligothiophenes, cyclo[12]thiophene (C[12]T), as the template.[27] The fullerenes can interact with the underlying cyclothiophenes at precisely the same position to form the 1 : 1 donor–acceptor (D–A) complexes. Scanning tunneling spectroscopy (STS) investigations reveal a bigger energy gap for the C[12]T–C_{60} complex due to the higher shift of the HOMO, while the position of the LUMO remains constant. Similar hierarchy replication based on charge-transfer between host and guest molecules was reported for fullerene and porphyrin derivatives.[28] 3-Cyanophenyl- and 3,5-di(*tert*-butyl)-phenyl-functionalized porphyrin (CP-DTBP porphyrin, Fig. 4a) can form a rectangular-shaped assembly on Ag(100) surfaces (Fig. 4b).[28] Upon deposition of porphyrin derivative molecules to complete surface coverage, the molecules arrange themselves into rows along the (110) direction of the underlying Ag(100) substrate. After deposition of C_{60} onto the molecular template, the rectangular array of aligned C_{60} pairs (intrapair distance of 2.3 nm) can be observed, which replicates the host lattice (Fig. 4c). The high thermal stability

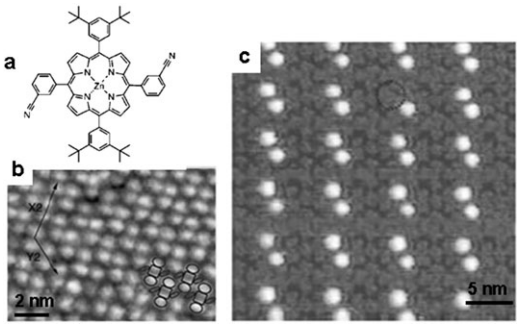

Fig. 4 (a) Molecular structure of 3-cyanophenyl- and 3,5-di(*tert*-butyl)phenyl-functionalized porphyrin (CP-DTBP porphyrin). (b) STM image of a full-coverage monolayer of CP-DTBP porphyrin sublimed on Ag(100); the distance between the centers of two neighboring molecular subunits is 2.4 ± 0.1 nm along the X2 direction and 1.5 ± 0.1 nm along the Y2 direction; the molecular rows along the direction X2 and Y2 cross each other at an angle of 126 ± 5°. (c) STM image of CP-DTBP porphyrin–C_{60} assembly; the circle indicates a C_{60} vacancy. (Reproduced with permission from ref. 28. Copyright 2004 Wiley-VCH Verlag GmbH & Co. KGaA).

and the long-range order of the C_{60} can be ascribed to the rather high porphyrin–fullerene interaction energy. The addressable supramolecular architectures result from a delicate balance between the fullerene–porphyrin interaction and conformational motion within the underlying porphyrin layer.

Another kind of template replication is widely pursued by using controlled inclusion of guest molecules. Tetraacidic azobenzene molecule (NN4A)[29] can exclusively form 2D porous Kagomé networks with two types of cavities with different size and symmetry through hydrogen bond interactions between carboxyl groups at the liquid–solid interface. The accommodation of fullerene molecules in the open Kagomé network was observed with high selectivity. C_{80} and $Sc_3N@C_{80}$ molecules can be trapped exclusively in the larger cavities, which implies appreciable site selectivity. In addition, as the metal atoms increase the electronegativity of the carbon cage, $Sc_3N@C_{80}$ shows enhanced interaction with the NN4A–graphite template.

Cooperative assembly with a flexible network as the template. Supramolecular networks with considerable flexibility could enrich the category of molecular architectures for guest molecule inclusion. The cooperative assembly of binary or tertiary molecular species enables hierarchical assembly at different levels. Recently, hierarchical assembly using multiple hydrogen bonds, or van der Waals interactions have been reported *via* cooperative assembly with flexible networks as templates.

Co-deposition of PTCDI and melamine on an Au(111) surface with a ratio of 3 : 4 leads to the formation of a chiral "pinwheel" structure at room temperature.[30] This result is in contrast to other reports that non-chiral honeycomb networks with a ratio of 3 : 2 at high temperature[26] or parallelogram network, also with a ratio of 3 : 2, are stable at room temperature.[31,32] This chiral pinwheel structure is hexagonal with a 37.8 ± 0.5 Å lattice parameter. The center of the pinwheel is composed of a melamine arrangement, where six melamine molecules form a chiral hexagon stabilized by

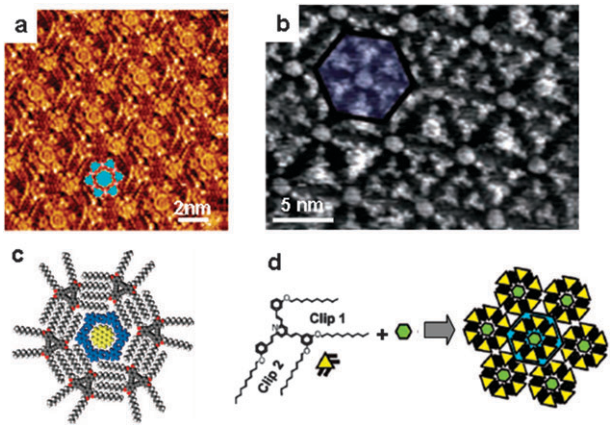

Fig. 5 (a) STM images of tri-component hierarchical architecture coronene–ISA–DBA at the 1-octanoic acid–graphite interface. A model of the coronene1–ISA6 cluster is overlaid on the image to guide the eye. The corresponding molecular model for the tri-component hierarchical assembly of coronene–ISA–DBA is illustrated in (c). (Reproduced with permission from ref. 33. Copyright 2008 American Chemical Society) (b) STM image after rearrangement of bi-clips (bifunctional molecules with a 2,4,6-tristyrylpyridine core) induced by addition of hexabenzocoronene and the scheme of the obtained hierarchical structure is shown in (d). (Reproduced with permission from ref. 12. Copyright 2007 Wiley-VCH Verlag GmbH & Co. KGaA).

double hydrogen bonds. This hexagon is surrounded by PTCDI pairs with one hydrogen bond formation between each inner PTCDI molecule and the melamine molecule.

The hierarchical assembly of coronene–isophthalic acid (ISA)[33] was reported as a hexagonal network with coronene surrounded by a cyclic hexamer of ISA molecules. The ISA hexamers are held together by double C=O···H–O hydrogen bonds between neighboring ISA molecules. At the higher level, the hexagonal coronene–ISA building blocks are close-packed through van der Waals interactions, which can be considered as the hierarchical model shown in Scheme 1d. More interestingly, this hierarchical assembly can be expanded into an even higher level of structure hierarchy by incorporating alkoxylated dehydrobenzo[12]annulene (DBA) molecules.[33] Ternary supramolecular networks of coronene–ISA–DBA demonstrated the hierarchical assembly at the liquid–solid interface following the host–guest strategy (Fig. 5a). The coronene–ISA hexagonal clusters fit perfectly into the hexagonal cavity formed by six DBA molecules (Fig. 5c). The first level of the ISA hexamer is dominated by hydrogen bonds, while the surrounding DBA honeycomb lattice is stabilized by van der Waals interactions at the second level.[33] The stabilization of the multilevel hierarchical assembly is due to the dynamic nature of the liquid–solid interface for equilibrium conditions of the complex pattern formation.

Common to the multi-component assemblies is that the introduction of guest species could generate appreciable structural transformation of the host networks. This effect has also been observed in hierarchical host–guest assemblies.[12,33] For the coronene–ISA system, coronene could induce the transformation of the zigzag linear pattern of ISA into hexagonal networks.[33] Another similar phenomenon was reported for the molecular clips based on a 2,4,6-tristyryl-pyridine core.[12] A linear zigzag configuration was observed for the molecules with two clips (di-clips), which permits the most compact packing. The addition of hexabenzocoronene (HBC) induced a structural transformation from linear assembly into six-membered hexagonal rings connected by crystallization of the alkyl chains (Fig. 5b).[12] Due to the absence of the outward-pointing clips, the assembly of the heterogeneous host–guest clusters reached another higher level by van der Waals interactions between the clusters into a hexagonal superlattice (Fig. 5d), which can be viewed as the hierarchical assembly structure illustrated in Scheme 1d.

3. Hierarchical levels with different symmetries

In contrast to the hierarchical assembly with similar symmetries discussed above, if the building blocks formed at the first level have asymmetrically distributed interactions, the hierarchical assembly with dissimilar symmetry would occur accordingly. In the case of a molecule schematically represented by a rectangular structure, as illustrated in Fig. 6a, the dominant interactions at both short sides will result in chain-like building blocks, followed by parallel packing of the molecular chains into double-chains or stripe-like patterns. One may notice that dominant interactions at long sides will also give rise to the double-chain stripe-like hierarchical assembly, which is principally similar to the chain-like assembly illustrated in Fig. 6a. If the interaction sites of the elemental building units are only at one long side or one short side, then the building blocks are predicted to consist of two basic units, followed by the packing of the rectangles into bigger rectangles or double-chains. If the interaction strength at both of the two short sides and the two long sides are the same, the asymmetric distribution of the interactions related to the shapes of the building blocks would lead to more complicated hierarchical assembly of interpenetrating networks (Fig. 7a). This simplified model based on interaction anisotropy could benefit studies, not only in 2D hierarchical assembly on the surface, but also in bulk materials ranging from biomaterials (such as DNA, proteins, peptides, *etc.*), copolymers, to π-conjugated disk-shaped molecules for columnar aggregates.

3.1 Hierarchical assemblies dominated by anisotropic interactions

Chain-like assemblies with dominant head-to-tail interactions. The chain-like hierarchical assemblies with dominant head-to-tail interactions can be realized by several kinds of interaction characteristics. If head-to-tail interactions (metal–organic coordination, hydrogen bonding, van der Waals interactions, *etc.*) are the dominant ones between molecules with rectangular shapes, chain-like building blocks could be expected (Fig. 6a). The triangular-shaped molecules with relatively strong interaction sites located at two sides could also form zigzag-shaped chains at the first level by hydrogen bonds or van der Waals interactions, which can be assigned to pseudo dominant head-to-tail interaction schematics (Fig. 6b–d). Anisotropic directional growth on pre-patterned

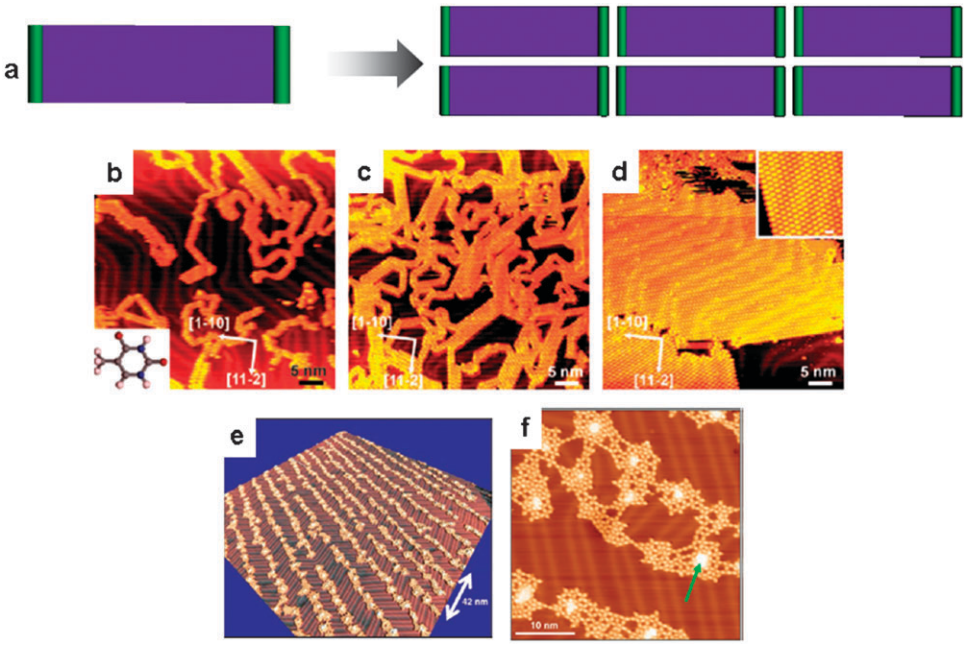

Fig. 6 (a) Schematic illustration of the chain-like assembly from elemental building units with rectangular structures. (b–d) STM images of thymine with increasing surface coverage. (b) 1D thymine filaments with random growth directions on the Au(111) surface at low surface coverage; the lower inset shows the chemical structure of a thymine molecule. (c) 1D thymine filaments and small islands correspond to an increased surface coverage. (d) STM image of extended 2D ordered thymine islands observed when the surface coverage is increased even further to ~0.3–0.4 monolayers. The inset shows a zoomed STM image of the 2D T island structure with high molecular resolution. (Reproduced with permission from ref. 38. Copyright 2007 Wiley-VCH Verlag GmbH & Co. KGaA). (e–f) illustrate the chain-like hierarchical assembly with the combination of nanopatterning and controlled localized reaction of TPA and Fe. Fe island is indicated by arrow. (Reproduced with permission from ref. 40. Copyright 2005 Wiley-VCH Verlag GmbH & Co. KGaA).

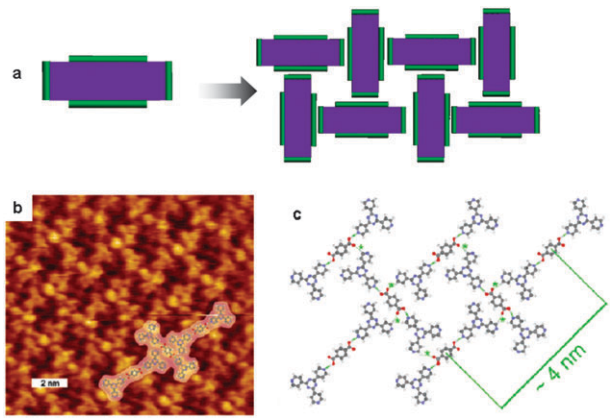

Fig. 7 (a) Schematic illustration of the interpenetrating network assembly dominated by the head-to-side interactions of the building blocks. (b) STM image of the hierarchical assembly of 1,3,5-tris-(4-pyridyl)-2,4,6-triazine and 1,4-benzenedicarboxylic acid (TPT and TPA) on a graphite surface. TPT molecules appear as bright, triangularly arranged features, whereas TPA appears as a single round feature. (c) Molecular model of the TPT–TPA interpenetrating network structure. The bold dashed green lines indicate the N···H–O hydrogen bonds between the elemental building units in TPT–TPA–TPT building blocks, and the fine green lines (additionally marked with asterisks) indicate weaker C–H···O hydrogen bonds between the TPT–TPA–TPT building blocks. (Reproduced with permission from ref. 45. Copyright 2005 American Chemical Society).

surfaces can also lead to chain-like hierarchical assembly over a large length scale (Fig. 6e–f).

Typical chain-like assemblies with dominant head-to-tail interactions between rectangular-shaped molecules were reported by Barth *et al.* for 4-[*trans*-2-(pyrid-4-yl-vinyl)]benzoic acid (PVBA) and 4-[(pyrid-4-yl-ethynyl)]benzoic acid (PEBA).[34] The predominant intermolecular interaction is head-to-tail hydrogen bonding, which accounts for stronger intrarow –COOH···N hydrogen bonds and promotes directional growth. The arrangement of the rows is dictated by the electrostatic interaction (which could also be viewed as weak hydrogen bonding) formation between the double-bonded carbonyl oxygen and the hydrogen atoms of adjacent molecules in neighboring rows.

Based on the assembling scenario illustrated in Fig. 6a, the long-range ordering and stabilization of one-dimensional (1D) coordination systems can also be facilitated by hierarchical interaction at the second level. 1D copper–pyridyl coordination chains on surfaces demonstrated a metastable phase with random spacing between neighboring copper–pyridyl rows and irregular chain lengths on Cu(100) surfaces at room temperature.[35] The strong metal–organic coordination interaction alone cannot lead to regular organization of these molecular chains into 2D or 3D ordering.[10] Long-range ordering and stabilization of the 1D copper–pyridyl coordination systems was realized with an additional molecular species. This hierarchical assembly can be achieved with strong metal–organic coordination at the first level, followed by ordering of the rows determined by the carboxylate hydrogen bond motif.

Hydrogen-bonded bi-component 1D supramolecular polymers with either a linear or a zigzag geometry were studied

by STM at the liquid–solid interface of graphite.[36] The ditopic molecular components comprise complementary hydrogen-bonding recognition groups like mortise-tenon joint, a Janus-type cyanuric wedge or barbituric wedge (ADA–ADA-array) for tenon and a corresponding (DAD–DAD-array) receptor unit as mortise. The physisorption of 1D bi-component hydrogen-bonded supramolecular polymers was observed by STM at surfaces, owing to the appropriate design of complementary building blocks linked by six hydrogen bonds at each node. The connecting molecules as tenon with flexible bridging components lead to a linear supramolecular polymer, while the rigid bridging components lead to zigzag type polymer-like assemblies. The polymers are laterally assembled at the second level through van der Waals interactions between the alkyl chains of the neighboring rows. This study could be beneficial for understanding the formation process of 1D supramolecular polymeric strands in solution by polyassociation through multiple hydrogen bonds.[37]

Dominant head-to-tail van der Waals interactions can also be utilized in the hierarchical assembly of the polymer-like assemblies at the first level. A rectangular shaped molecular clip[12] is designed for an elongated core with two 2,4,6-tristyryl-pyridine units connected by a divinylbenzene group, and two clips located at the head and tail sides. A polymer-like 1D assembly was observed due to the crystallization of the alkyl chains at both ends. The polymer chains are packed into 2D patterns by van der Waals interactions between neighboring chains.

As mentioned above, the triangular-shaped molecules with relatively strong interactions located at two sides can also lead to zigzag chain-like assemblies. The hydrogen bonds between two sides of the triangle of ISA molecules facilitate the zigzag close-packing of the molecules into chain-like assemblies, followed by chain arrangement driven by van der Waals interactions between neighboring chains.[33] The van der Waals interactions between di-clips based on the triangular 2,4,6-tristyrylpyridine core also gives rise to the zigzag packing of the molecules due to the dominant head-to-tail interactions.[12] It has been demonstrated that the thymine molecules adsorbed on an Au(111) surface undergo a two-level hierarchical assembly process.[38] Initially at low coverage, strong hydrogen bonds through the carbonyl and imino groups steer the growth of 1D filaments of thymine molecules (Fig. 6b). At the second stage, higher coverage of thymine on the gold surface renders the formation of 2D thymine islands *via* van der Waals interactions between the methyl groups (Fig. 6c and d). The influence of the alkyl substituent on the hierarchical interactions has been systematically investigated elsewhere by introducing van der Waals interactions into the assembly system.[39] Interestingly, by using STM manipulation with high-voltage pulses applied during scanning, the hierarchy of bond strengths can by directly probed by selectively breaking up the van der Waals interactions, resulting in the lateral disassembly of the 2D thymine islands into 1D thymine filaments.[38] This technique of selective disassembly of hierarchical self-assembled molecular structures into their lower-level supramolecular building blocks might offer valuable new insights into the nature of interactions involved in hierarchical assemblies.

Polymer chain-like hierarchical assemblies can also be obtained over a large length scale by the combination of nanopatterning and controlled metal–organic complexation. Regularly spaced metal–organic coordination ribbons were reported with the confinement of the reconstructed terrace of Au(111) substrate.[40] Regular lattices of transition metal dots can be formed by depositing small amounts of cobalt or iron on Au(111) at room temperature due to the preferred nucleation of metal islands at the elbow sites of the reconstructed Au(111) surface. The localized reactions between metal island and terephthalic acid molecules (TPA, 1,4-benzenedicarboxylic acid) facilitate the metal–organic complex nanodot arrays owing to the limited diffusion of the complex and mobility of the TPA molecules on a bare Au(111) surface. The connection between the localized complex islands enables the regularly spaced ribbons with mixed metal–organic coordination and hydrogen bond interactions (Fig. 6e and f). The favorable connection along the elbows could be ascribed to the shortest distance between metallic dots, and the directional molecular transport and orientations induced by the substrate reconstruction.

Stripe-like assemblies dominated by side–side interactions. The interaction anisotropy between molecular sides is similar to the head-to-tail configurations, which are schematically shown in Fig. 6a. The interaction sites located at the long sides and the dominant side-to-side interactions between rectangular molecules lead to stripe-like assemblies. As an example, the evolution of multilevel ordering of bis-urea-substituted toluene on an Au(111) surface was studied by low temperature STM.[10] The formation of the stripe-like patterns is controlled by specific hydrogen bonds between adjacent molecules at the first level. The pairing of the polymer chains is steered by lateral van der Waals interactions between the alkyl chains at one side. The weak interaction between the molecule and substrate also contributes to the large-area pattern resulting from packing of the double polymer chains.

In a UHV study at low temperature, it was demonstrated that by adjusting the dipole–dipole interaction *via* functional groups of cyanophenyl porphyrin, a 1D molecular wire structure (*trans*-BCTBPP, with two cyano substitutions with *cis* positions) could be achieved.[41] The substitution scheme is designed to modulate the dipole–dipole and van der Waals interactions. The driving interactions could be associated with the dipole–dipole interactions for pairing of the molecules at the first level. As a result, the molecular pairs are packed into the observed 1D molecular wires.

Binary molecular motifs connected by hydrogen bonds have been constructed in a number of studies. A hydrogen-bonded motif formed by TMA and alcohols could generate a lamellar structure with alternating hydrophilic and hydrophobic regions, in which the periodicity is proportional to the length of the alcohol.[42] Binary supramolecular assemblies of TMA–4,4′-bipyridine can be formed by heterogeneous N···H–O hydrogen bonds.[43] The molecular motifs of acid–bipyridine–acid building blocks are connected into stripe-like building blocks *via* inter-motif hydrogen bonds.[43] The stripes can be stabilized themselves on the surface or more ordered and stabilized into large patterns *via* inter-row hydrogen bonds.

The hierarchical assembly characteristics could also be modulated by the substrate electric potentials using electrochemical STM.[44] The ISA derivative, ISA16 with alkyl chains attached to ISA molecules, first assemble into a close-packed lamellae structure at substrate potentials close to zero. With the increasing substrate potential, the close-packed lamellae structure disassembles into individual rows at relatively high potential, and eventually becomes dispersed single molecules at high substrate potentials. This phenomenon may be associated with the increased electrostatic repulsion between neighboring rows owing to the deprotonation of the ISA moiety at higher positive potentials.

Assemblies dominated by head-to-side interactions. As illustrated in Fig. 7a, if the interaction strengths in the two perpendicular directions are the same, the shapes of the building blocks will lead to the hierarchical assembly of an interpenetrating network. Similar to the molecular motifs of TMA–4,4′-bipyridine, a binary molecular motif can be formed by TPA and 1,3,5-tris(4-pyridyl)-2,4,6-triazine (TPT) with a ratio of TPA : TPT = 1 : 2 and connected by N···H–O hydrogen bonds between nitrogen atoms of TPT and carboxylic hydrogen atoms of TPA.[45] These motifs subsequently form a supramolecular network *via* hydrogen bonds between the C═O of the carboxyl groups on TPA and C–H adjacent to the N atoms on TPT. Intermolecular N···H–O hydrogen bonds are the predominant interactions for the formation of binary motifs at the first level. The quadratic interpenetrating network is formed at the second level using weaker C═O···H–C hydrogen bonds with a head-to-side configuration (Fig. 7b and c).

3.2 Hierarchical assemblies with dominant chiral interactions and recognition

Homochiral assembly systems have been extensively pursued for their relevance to enantioselective synthesis and separation. It is highly desirable for controlled chirality conservation from molecules to assembled building blocks, even to crystalline-like architectures. Several reports have shown homochiral networks formed by hydrogen-bonded DNA bases,[17] metal–organic coordination-bonded hierarchical assemblies,[19,20] and hydrogen-bonded multi-component chiral pinwheel structures,[30] *etc*. Here, in this section, we will briefly review the chirality effects on the 2D hierarchical supramolecular structures.

Chiral trimers from achiral monomer, tripod-shaped bromo adamantane trithiol (BATT), can be formed on Au(111) surfaces at 4.7 K.[46] The subsequent assembly of the chiral trimers leads to chiral hexagonal molecular clusters. Chiral trimer formation at the first hierarchical level can be attributed to distortion of the molecular structure due to the intermolecular interaction between S atoms. The higher level assembly into hexagonal architectures is associated with chiral interaction and recognition. The chirality effect at the second level assembly could be manifested by the growth process, in which the hexagons from initially a racemic mixture of hexagons evolved into enantiomeric domains with increasing surface coverage.

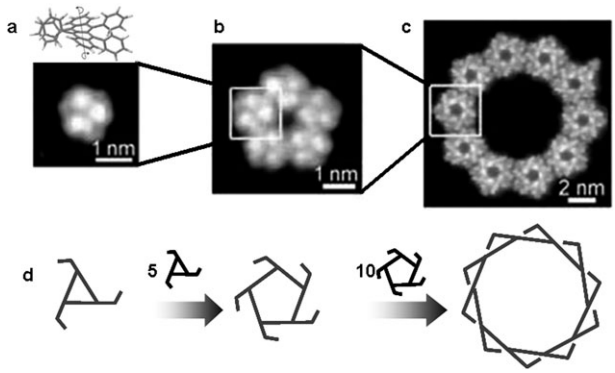

Fig. 8 The hierarchy and conservation of chirality in the spontaneous two-dimensional supramolecular assembly of 5,6,11,12-tetraphenylnaphthacenen (rubrene) molecules. (a–c) STM images representing the three generations of the two-leveled hierarchical assembly. The molecular structure of rubrene is presented corresponding to the STM image of a single molecule in (a). (d) The enantioselective assembly from *L*-type monomers to *L*-type pentagons and further on to *L*-type decagons. (Reproduced with permission from ref. 47. Copyright 2005 Wiley-VCH Verlag GmbH & Co. KGaA).

Chiral molecule 5,6,11,12-tetraphenylnaphthacene (rubrene, $C_{42}H_{28}$) (Fig. 8a) can self-assemble into a pentagonal supermolecule with a radius of 1 nm (Fig. 8b).[47] The observed self-assembly is the result of an interplay of van der Waals interactions and C–H···π hydrogen bonds. Hierarchical supramolecular self-assembly at the second level leads to either enantiomeric zigzag supramolecular chains or enantiomeric decagons (Fig. 8c) with the pentagonal supermolecules as building blocks. Both of the hierarchical assemblies of supramolecular chains and decagons conserve the same chirality as the chiral rubrene molecule and the chiral pentagonal supermolecule (Fig. 8d), which can be ascribed to the chirality-dependent rotation of the building blocks. A similar chiral conservation was reported for the hierarchical chirality of *R*- or *S*-alanine on Au(111) surfaces.[48] Alanine molecules self-organize to form chiral clusters of six or eight molecules at the surface with chiral channels between the chiral clusters. These clusters and channels further self-assemble into a chiral array at the second level.

Chiral expression of a racemic mixture of 8-nitrospiropyran (SP8) molecules on Au(111) surfaces shows a mirror-imaged chiral domain on Au(111) through hierarchical assembly.[49] Antiparallelly packed homochiral dimers of *R*-SP8 or *S*-SP8 are first formed due to the inter-adsorbate van der Waals as well as C–H···O and C–H···π interactions. Chiral quatrefoils as chiral building blocks for the enantiomeric networks can be obtained at the second level by packing of two *R*-dimers and two *S*-dimers.

4. Environmental effects on hierarchical assembly

As is well known, molecular assembly is a process with a delicate balance between adsorbate–adsorbate, adsorbate–substrate and adsorbate–environment interactions. The hierarchical assembly on surfaces could be influenced by environmental conditions, such as UHV conditions, solvent polarity at the solid–liquid interface, thermal effects, substrate effects due to the charge transfer between molecules and substrate, substrate registration effect, *etc*.

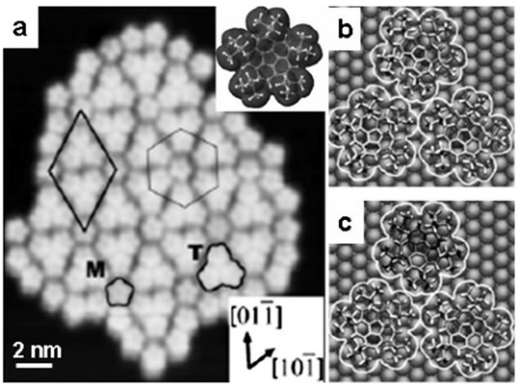

Fig. 9 (a) STM image of hierarchical assembly of penta-*tert*-butylcorannulene (PTBC) on Cu(111). M indicates a single PTBC molecule (monomer), and T indicates an assembly of three molecules (trimer). The rhombus and the hexagon delineate a unit cell and its seven-molecule basis. The inset shows the van der Waals surface of PTBC. (b) and (c) Optimized adsorption configurations of homochiral and heterochiral PTBC trimer, respectively. (Reproduced with permission from ref. 50. Copyright 2009 Wiley-VCH Verlag GmbH & Co. KGaA).

4.1 Substrate effects on hierarchical assembly

The van der Waals and electronic interactions between adsorbed molecules with π-electron systems and substrates are important in determining the adsorption registry and subsequent assembly behavior. A substrate-induced symmetry mismatch for hierarchical assembly was reported recently for a corannulene derivative (penta-*tert*-butylcorannulene, PTBC) with five-fold symmetry.[50] PTBC trimers on Cu(111) surfaces (Fig. 9a) were formed at the first level by molecule–substrate interactions, which can be considered as a way to generate structures with a symmetry compatible with that of the substrate (Fig. 9b and c). The close-packing of the three-fold-symmetric trimers at the second level gives rise to the hexagonal networks with cavities accommodating one monomer (Fig. 9a).

Another example of the substrate effect is the 2D porphyrin-based supramolecular porous network structure on Ag(111) and Ag(100) surfaces.[28,51] Hierarchical hexagonal arrangements of porphyrin trimers can be obtained on Ag(111) surfaces.[51] At the first level, the dipole–dipole interaction is predominant for the formation of the porphyrin trimers. Then, the van der Waals interaction between the 3,5-di(*tert*-butyl)-phenyl substituents and the close-packing of the trimers leads to the hexagonal arrangement of the trimeric building blocks. Predicted from the interaction sites on this porphyrin derivative (similar to Fig. 6a), chain-like assembly structures could also be possible. So, the hierarchical hexagonal pattern should be induced by the six-fold symmetry of the Ag(111) surface.[51] Investigations of the same porphyrin derivative on

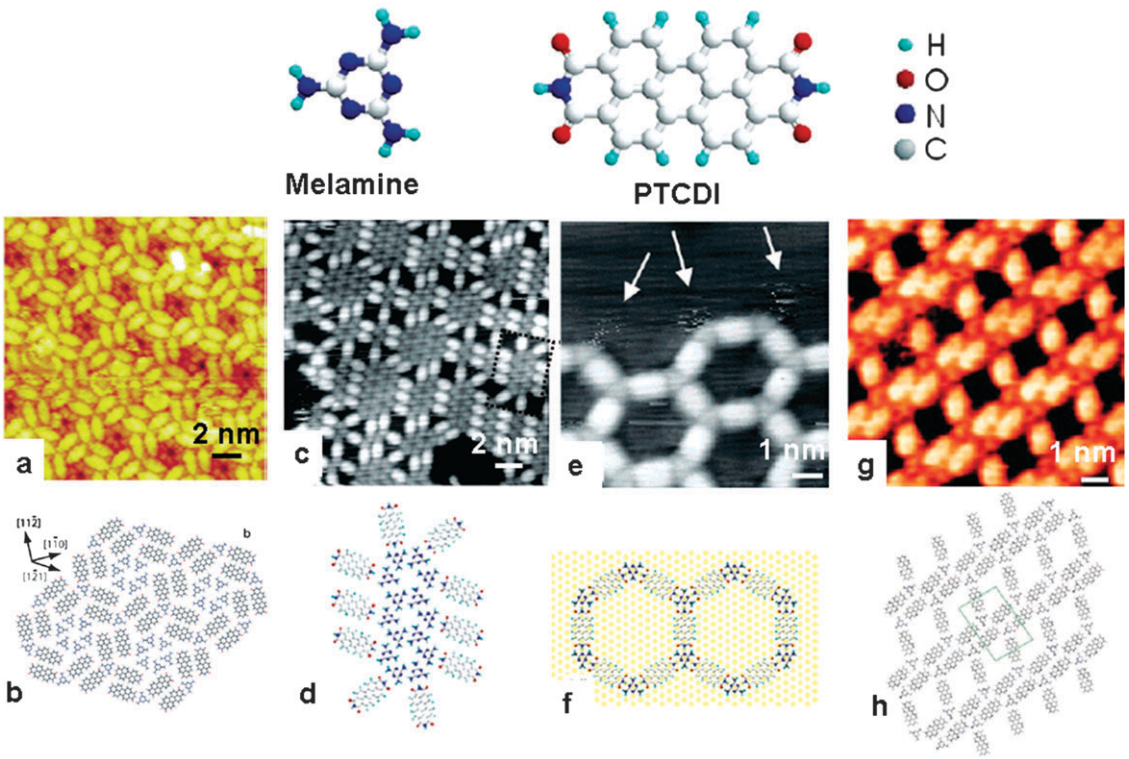

Fig. 10 Thermal effects on the hierarchical assembly of melamine–PTCDI on an Au(111) surface. (a) and (b) Chiral pinwheel structure at room temperature. (Reproduced with permission from ref. 30. Copyright 2008 The Royal Society of Chemistry.) (c) and (d) Chiral structures with smaller melamine islands with PTCDI molecules adsorbed around their edges at 50 °C. (Reproduced with permission from ref. 53. Copyright 2006 American Chemical Society.) (e) and (f) Hexagonal networks at 60–80 °C. (Reproduced with permission from ref. 53. Copyright 2006 American Chemical Society.) (g) and (h) Parallelogram arrangement at 150 °C. (Reproduced with permission from ref. 32. Copyright 2008 The Royal Society of Chemistry).

Ag(100) surfaces showed a nearly rectangular unit cell.[28] Such complementary investigations further confirmed the substrate-induced symmetry mismatch for hierarchical assemblies.

4.2 Solvent effects on hierarchical assembly

Solvent effects, such as solvent polarity, hydrogen bond-formation capability, solubility and solvent chirality, on hierarchical assembly would enable dynamically controlled assembly of the molecular architectures.[9] When hydrogen bonding is the main driving force for the hierarchical assemblies, the solvent polarity and hydrogen bond-formation capability could appreciably influence the assembly architectures.

Recently, 2D organization of chiral rosette structures self-assembled from achiral diamino triazine oligo-(*p*-phenylene-vinylene) oligomer (A-OPV4T) was reported in a chiral solvent system.[52] At the first hierarchical level, the rosette structures of A-OPV4T are formed by multiple hydrogen bonds between diamino triazine groups of the neighboring molecules. At the second level, van der Waals interactions between the rosette structures lead to the hexagonal arrangements following the model shown in Scheme 1b. The counterclockwise rotating rosettes are more favored in solvent (*R*)-1-phenyl-1-octanol than in (*S*)-1-phenyl-1-octanol, which can be possibly ascribed to the transient interaction of the chiral solvents through hydrogen bonds with the unbound nitrogen atoms in the rosettes with particular handedness. Upon desolvation, rosettes with a particular handedness are formed on the surface. In addition to the expression of chirality at the level of the rosettes, the self-assembly of the rosettes is also chiral and solvent-dependent.

4.3 Thermal effects on hierarchical assembly

Thermal annealing is another factor for controlled assembly, where one can increase temperature to increase the mobility and collision possibility of molecules on the surface. Thermal effects on hierarchical assemblies have been discussed above for metal–organic coordination networks,[20] and hydrogen-bonded supramolecular assemblies.[30–32,53] This effect has also been widely used for delicate controlling of the hierarchical

Table 1 Symmetries and interactions involved in hierarchical assemblies at different levels[a]

	First hierarchical level		Second hierarchical level			
Elemental building units	Symmetry	Interactions	Symmetry	Interactions	Environmental conditions	Schematic representation
tmla/Fe, TMA/Fe	Square	MOC	Square	HB	UHV[19,20b]	Scheme 1a
Guanine	Square	HB	Square	HB	UHV[17]	Scheme 1a
Monodendron **1**, Monodendron **2**	Rhombic	HB	Rhombic	vdWs	Ambient or liquid–solid interface[13,14]	Scheme 1a
Monodendron **3**, A-OPV4T	Hexagonal	HB	Hexagonal	vdWs	Ambient or liquid–solid interface[15,52]	Scheme 1b
Monodendron **4**	Parallelogram	DD	Parallelogram	vdWs	Ambient[15]	Scheme 1c
Mono-clip	Parallelogram	vdWs	Parallelogram	vdWs	Liquid–solid interface[12]	Scheme 1c
3,3′-BTP	Hexagonal	HB	Hexagonal	HB, vdWs	Liquid–solid interface[16]	Scheme 1d
Coronene/ISA	Hexagonal	HB	Hexagonal	vdWs	Liquid–solid interface[33]	Scheme 1d
Di-clips/HBC	Hexagonal	vdWs	Hexagonal	vdWs	Liquid–solid interface[12]	Scheme 1d
BTP-PTCBI/Zn^{2+}	Triangular	MOC	Hexagonal	vdWs	Liquid–solid interface[22]	Scheme 1e
M/CA	Triangular	HB	Hexagonal	HB	UHV[18]	Scheme 1f
PTCDI/M/C_{60}	Hexagonal	HB	Hexagonal	Template	UHV[26]	[c]Rigid template
C[12]T/C_{60}	Hexagonal	vdWs	Hexagonal	Charge transfer	Liquid–solid interface[27]	[c]Rigid template
CP-DTBP porphyrin/C_{60}	Row	DD, vdWs	Rows of dimers	Charge transfer	UHV[28]	[c]Rigid template
NN4A/$Sc_3N@C_{80}$	Kagomé	HB	Hexagonal	Template	Liquid–solid interface[29]	[c]Rigid template
PTCDI/M	Hexagonal	HB	Hexagonal	HB	UHV[30]	[b]Flexible template
Coronene/ISA/DBA	Hexagonal	HB	Hexagonal	vdWs	Liquid–solid interface[33]	[c]Flexible template
PVBA, PEBA, Cu/pyridyl	Chain	MOC	Double-chain or aligned chains	HB	UHV[34,35]	Fig. 6a
Tenon/mortise	Chain	HB	Aligned chains	vdWs	Liquid–solid interface[36]	Fig. 6a
Di-clips	Chain	vdWs	Aligned chains	vdWs	Liquid–solid interface[12]	Fig. 6a
TMA/alcohols, TMA/4,4′-bipyridine	Stripe	HB	Aligned stripes	HB	Ambient or liquid–solid interface[42,43]	Fig. 6a
TPA/TPT	Rectangular	HB	Interpenetrating networks	HB	Liquid–solid interface[45]	Fig. 7a

[a] Abbreviations in Table 1: HB: hydrogen bond; vdWs: van der Waals interaction; MOC: metal–organic coordination; DD: dipole–dipole interaction; tmla: 1,2,4-benzenetricarboxylic acid; TMA: 1,3,5-benzenetricarboxylic acid, trimesic acid; ISA: isophthalic acid; A-OPV4T: achiral diamino triazine oligo-(*p*-phenylenevinylene) oligomer; mono-clip and di-clips: alkyl functionalized 2,4,6-tristyrylpyridine cores, mono-clip with alkyl chains at one side and di-clips at two sides of the triangular core; 3,3′-BTP: 2-phenyl-4,6-bis(6-(pyridine-3-yl)-4-(pyridine-3-yl)pyridine-2-yl) pyrimidine; DBA: alkoxylated dehydrobenzo[12]annulene; HBC: hexabenzocoronene; BTP-PTCBI: bis(terpyridine)-functionalized perylene tetracarboxylic bisimide; M: melamine; CA: cyanuric acid; PTCDI: perylenetetracarboxylic-diimide; C[12]T: cyclo[12]thiophene; CP-DTBP porphyrin: 3-cyanophenyl and 3,5-di(*tert*-butyl)phenyl-functionalized porphyrin; NN4A: tetraacidic azobenzene; PVBA: 4-[*trans*-2-(pyrid-4-yl-vinyl)]benzoic acid; PEBA: 4-[(pyrid-4-yl-ethynyl)]-benzoic acid; tenon and mortise: cyanuric wedge or barbituric wedge (ADA–ADA-array) as tenon and a corresponding (DAD–DAD-array) receptor unit as mortise; TPA: 1,4-benzenedicarboxylic acid, terephthalic acid; TPT: 1,3,5-tris-(4-pyridyl)-2,4,6-triazine. [b] The third level hierarchical assembly also follows the same symmetry as the first and second levels. [c] Please refer to the corresponding references for schematic representations of templated hierarchical assemblies.

assembly of the donor–acceptor structures for molecular electronics, functionalized polymers, *etc*.

The hierarchical assembly of nanoporous metal–organic coordination networks can be tuned by thermal annealing temperatures.[20] At the same molecular stoichiometry of TMA to Fe, which is Fe coverage = 0.06 ML and TMA coverage = 0.8 ML, the first level hierarchical assembly of the center building blocks can be achieved at 300 K (Fig. 3a). Upon further annealing the substrate to 400 K, the formation of extended nanocavity arrays at the third level can be obtained with homochiral *R* or *S* domains consisting of pure enantiomers (Fig. 3c).

Hydrogen-bonded bi-component supramolecular assemblies of PTCDI and melamine reveal a high dependence on the annealing temperature of the substrate. After deposition of PTCDI and melamine molecules onto the Au(111) surface at room temperature, chiral pinwheel structures can be achieved without post-sample annealing (Fig. 10a and b).[30] The detailed description of the pinwheel supramolecular structure has been discussed above. With the sample annealing at around 50 °C, the intermixing between melamine and PTCDI gives rise to the chiral structures with smaller melamine islands with PTCDI molecules adsorbed around their edges and forming a bridge to neighboring islands (Fig. 10c and d).[53] The chiral pinwheel structure can be considered as part of this mixing chiral structures with perfect stoichiometry. Subsequent annealing in the range of 60–80 °C results in the formation of hexagonal networks (Fig. 10e and f),[53] which is similar to the networks on Ag/Si(111)-$\sqrt{3} \times \sqrt{3}$ R30° surface.[26] By annealing the sample at higher temperatures (Fig. 10g and h), ~90 °C[31] or 150 °C,[32] the hexagonal networks can be converted into a parallelogram arrangement. The dependence of the PTCDI–melamine networks may be associated with their high mobility on the gold surface and the different configurations of the multiple hydrogen bonds between the two molecules.

5. Conclusion

This tutorial review has summarized the hierarchical assemblies on surfaces relating to various interactions associated with the hierarchical levels. The dominant interactions and symmetries of the building blocks at different levels for hierarchical assemblies have been outlined in Table 1. The simplified structural building units of triangles and rectangles could be expanded into polygons for the hierarchical assembly of nearly all kinds of elemental building units or building blocks. Other possible hierarchical assemblies involving additional interaction types, such as steric interactions, electrostatic interactions, *etc*. are not included in this review. The incorporation of these non-directional interactions will render appreciably more complexity in the assembling characteristics. The reported works would be highly beneficial to research endeavors of constructing functional molecular architectures.

Acknowledgements

Prof. F. Besenbacher and Dr W. Xu are greatly acknowledged for their kind help in providing original figures.

References

1 N. C. Seeman, *Nature*, 2003, **421**, 427–431.
2 R. V. Ulijn and A. M. Smith, *Chem. Soc. Rev.*, 2008, **37**, 664–675.
3 H. M. Keizer and R. P. Sijbesma, *Chem. Soc. Rev.*, 2005, **34**, 226–234.
4 L. Piot, C. Marie, X. Feng, K. Müllen and D. Fichou, *Adv. Mater.*, 2008, **20**, 1–5.
5 O. Ikkala and G. ten Brinke, *Chem. Commun.*, 2004, 2131–2137.
6 F. Cicoira, C. Santato and F. Rosei, *Top. Curr. Chem.*, 2008, **285**, 203–267.
7 T. Kudernac, S. Lei, J. A. A. W. Elemans and S. De Feyter, *Chem. Soc. Rev.*, 2009, **38**, 402–421.
8 J. V. Barth, G. Costantini and K. Kern, *Nature*, 2005, **437**, 671–679.
9 Y. L. Yang and C. Wang, *Curr. Opin. Colloid Interface Sci.*, 2009, **14**, 135–147.
10 F. Vonau, D. Suhr, D. Aubel, L. Bouteiller, G. Reiter and L. Simon, *Phys. Rev. Lett.*, 2005, **94**, 066103.
11 G. M. Whitesides and B. Grzybowski, *Science*, 2002, **295**, 2418–2421.
12 D. Bléger, D. Kreher, F. Mathevet, A.-J. Attias, G. Schull, A. Huard, L. Douillard, C. Fiorini-Debuischert and F. Charra, *Angew. Chem., Int. Ed.*, 2007, **46**, 7404–7407.
13 P. Wu, Q. Fan, G. Deng, Q. Zeng, C. Wang and C. Bai, *Langmuir*, 2002, **18**, 4342–4344.
14 W. Mamdouh, H. Uji-i, J. S. Ladislaw, A. E. Dulcey, V. Percec, F. C. De Schryver and S. De Feyter, *J. Am. Chem. Soc.*, 2006, **128**, 317–325.
15 P. Wu, Q. Fan, Q. Zeng, C. Wang, G. Deng and C. Bai, *ChemPhysChem*, 2002, **3**, 633–637.
16 C. Meier, K. Landfester, D. Künzel, T. Markert, A. Groβ and U. Ziener, *Angew. Chem., Int. Ed.*, 2008, **47**, 3821–3825.
17 R. Otero, M. Schöck, L. M. Molina, E. Lægsgaard, I. Stensgaard, B. Hammer and F. Besenbacher, *Angew. Chem., Int. Ed.*, 2005, **44**, 2270–2275.
18 W. Xu, M. Dong, H. Gersen, E. Rauls, S. Vázquez-Campos, M. Crego-Calama, D. N. Reinhoudt, I. Stensgaard, E. Laegsgaard, T. R. Linderoth and F. Besenbacher, *Small*, 2007, **3**, 854–858.
19 A. Dmitriev, H. Spillmann, M. Lingenfelder, N. Lin, J. V. Barth and K. Kern, *Langmuir*, 2004, **20**, 4799–4801.
20 H. Spillmann, A. Dmitriev, N. Lin, P. Messina, J. V. Barth and K. Kern, *J. Am. Chem. Soc.*, 2003, **125**, 10725–10728.
21 P. Gambardella, S. Stepanow, A. Dmitriev, J. Honolka, F. M. F. de Groot, M. Lingenfelder, S. Sen Gupta, D. D. Sarma, P. Bencok, S. Stanescu, S. Clair, S. Pons, N. Lin, A. P. Seitsonen, H. Brune, J. V. Barth and K. Kern, *Nat. Mater.*, 2009, **8**, 189–193.
22 V. Stepanenko and F. Würthner, *Small*, 2008, **4**, 2158–2161.
23 J. A. A. W. Elemans and S. De Feyter, *Soft Matter*, 2009, **5**, 721–735.
24 A. Dmitriev, N. Lin, J. Weckesser, J. V. Barth and K. Kern, *J. Phys. Chem. B*, 2002, **106**, 6907–6912.
25 S. J. H. Griessl, M. Lackinger, F. Jamitzky, T. Markert, M. Hietschold and W. M. Heckl, *Langmuir*, 2004, **20**, 9403–9407.
26 J. A. Theobald, N. S. Oxtoby, M. A. Phillips, N. R. Champness and P. H. Beton, *Nature*, 2003, **424**, 1029–1031.
27 E. Mena-Osteritz and P. Bäuerle, *Adv. Mater.*, 2006, **18**, 447–451.
28 D. Bonifazi, H. Spillmann, A. Kiebele, M. de Wild, P. Seiler, F. Cheng, H.-J. Güntherodt, T. Jung and F. Diederich, *Angew. Chem., Int. Ed.*, 2004, **43**, 4759–4763.
29 M. Li, K. Deng, S.-B. Lei, Y.-L. Yang, T.-S. Wang, Y.-T. Shen, C.-R. Wang, Q.-D. Zeng and C. Wang, *Angew. Chem., Int. Ed.*, 2008, **47**, 6717–6721.
30 F. Silly, A. Q. Shaw, M. R. Castella and G. A. D. Briggs, *Chem. Commun.*, 2008, 1907–1909.
31 P. A. Staniec, L. M. A. Perdigão, A. Saywell, N. R. Champness and P. H. Beton, *ChemPhysChem*, 2007, **8**, 2177–2181.
32 F. Silly, A. Q. Shaw, K. Porfyrakis, J. H. Warner, A. A. R. Watt, M. R. Castell, H. Umemoto, T. Akachi, H. Shinohara and G. A. D. Briggs, *Chem. Commun.*, 2008, 4616–4618.
33 S. Lei, M. Surin, K. Tahara, J. Adisoejoso, R. Lazzaroni, Y. Tobe and S. De Feyter, *Nano Lett.*, 2008, **8**, 2541–2546.

34 J. V. Barth, J. Weckesser, G. Trimarchi, M. Vladimirova, A. De Vita, C. Cai, H. Brune and P. Günter K. Kern, *J. Am. Chem. Soc.*, 2002, **124**, 7991–8000.
35 A. Langner, S. L. Tait, N. Lin, R. Chandrasekar, M. Ruben and K. Kern, *Angew. Chem., Int. Ed.*, 2008, **47**, 8835–8838.
36 A. Ciesielski, G. Schaeffer, A. Petitjean, J.-M. Lehn and P. Samorí, *Angew. Chem., Int. Ed.*, 2009, **48**, 2039–2043.
37 V. Berl, M. Schmutz, M. J. Krische, R. G. Khoury and J.-M. Lehn, *Chem.–Eur. J.*, 2002, **8**, 1227–1244.
38 W. Xu, R. E. A. Kelly, R. Otero, M. Schöck, E. Lægsgaard, I. Stensgaard, L. N. Kantorovich and F. Besenbacher, *Small*, 2007, **3**, 2011–2014.
39 W. Xu, M. Dong, H. Gersen, E. Rauls, S. Vázquez-Campos, M. Crego-Calama, D. N. Reinhoudt, E. Lægsgaard, I. Stensgaard, T. R. Linderoth and F. Besenbacher, *Small*, 2008, **4**, 1620–1623.
40 S. Clair, S. Pons, H. Brune, K. Kern and J. V. Barth, *Angew. Chem., Int. Ed.*, 2005, **44**, 7294–7297.
41 T. Yokoyama, S. Yokoyama S, T. Kamikado, Y. Okuno and S. Mashiko, *Nature*, 2001, **413**, 619–621.
42 K. G. Nath, O. Ivasenko, J. A. Miwa, H. Dang, J. D. Wuest, A. Nanci, D. F. Perepichka and F. Rosei, *J. Am. Chem. Soc.*, 2006, **128**, 4212–4213.
43 M. Li, Y.-L. Yang, K.-Q. Zhao, Q.-D. Zeng and C. Wang, *J. Phys. Chem. C*, 2008, **112**, 10141–10144.
44 A. S. Klymchenko, S. Furukawa, K. Müllen, M. Van der Auweraer and S. De Feyter, *Nano Lett.*, 2007, **7**, 791–795.
45 L. Kampschulte, S. Griessl, W. M. Heckl and M. Lackinger, *J. Phys. Chem. B*, 2005, **109**, 14074–14078.
46 S. Katano, Y. Kim, H. Matsubara, T. Kitagawa and M. Kawai, *J. Am. Chem. Soc.*, 2007, **129**, 2511–2515.
47 M.-C. Blüm, E. Cavar, M. Pivetta, F. Patthey and W.-D. Schneider, *Angew. Chem., Int. Ed.*, 2005, **44**, 5334–5337.
48 S. M. Barlow, S. Louafi, D. Le Roux, J. Williams, C. Muryn, S. Haq and R. Raval, *Langmuir*, 2004, **20**, 7171–7176.
49 T. Huang, Z. P. Hu, B. Wang, L. Chen, A. D. Zhao, H. Q. Wang and J. G. Hou, *J. Phys. Chem. B*, 2007, **111**, 6973–6977.
50 O. Guillermet, E. Niemi, S. Nagarajan, X. Bouju, D. Martrou, A. Gourdon and S. Gauthier, *Angew. Chem., Int. Ed.*, 2009, **48**, 1970–1973.
51 H. Spillmann, A. Kiebele, M. Stöhr, T. A. Jung, D. Bonifazi, F. Cheng and F. Diederich, *Adv. Mater.*, 2006, **18**, 275–279.
52 N. Katsonis, H. Xu, R. M. Haak, T. Kudernac, Ž. Tomović, S. George, M. Van der Auweraer, A. P. H. J. Schenning, E. W. Meijer, B. L. Feringa and S. De Feyter, *Angew. Chem., Int. Ed.*, 2008, **47**, 4997–5001.
53 L. M. A. Perdigo, E. W. Perkins, J. Ma, P. A. Staniec, B. L. Rogers, N. R. Champness and P. H. Beton, *J. Phys. Chem. B*, 2006, **110**, 12539–12542.